RSC Advances

ROYAL SOCIETY OF CHEMISTRY

www.rsc.org/advances

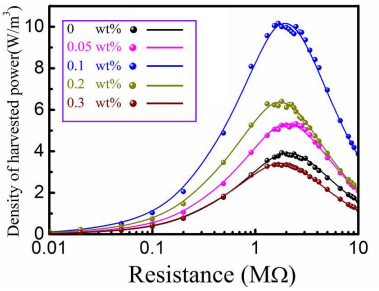

Mechanism clarification of the phase transformation in the three stages, i.e. initial crystallization, stretching and poling.

Cite this: DOI: 10.1039/c0xx00000x

www.rsc.org/xxxxxx

PAPER

Improvement of the piezoelectricity of PVDF-HFP using AgNWs

Liangke Wu,[a,b] Guiwen Huang,[c] Ning Hu,*[a] Shaoyun Fu,[c] Jianhui Qiu,[d] Zhongchang Wang,[e] Ji Ying,[b] Zichen Chen,[b] Weiguo Li,[a] and Shan Tang[a]

Received (in XXX, XXX) XthXXXXXXXXX 20XX, Accepted Xth XXXXXXXXX 20XX

DOI: 10.1039/b000000x

In order to improve the piezoelectricity of poly(vinylidene fluoride-co-hexafluoropropylene)(PVDF-HFP), we added various contents of silver nanowires (AgNWs) into PVDF-HFP and N,N-dimethylformamide (DMF) solution to prepare composite films. Stretching and poling were applied to the films to induce the formation of polar *β*-phase and reorientation of the dipole moment. The crystal structure of the films was investigated by polarized optical microscopy (POM), Fourier transform infrared spectroscopy (FTIR) and differential scanning calorimetry (DSC). The obtained results showed that the phase transformation mainly occurred in stretching and the reorientation of dipole moment was attributed to poling. It was also concluded that the AgNWs played a role as nucleate agents in the *β*-phase formation and the phase transformation. The piezoelectricity was also evaluated by the output voltage and harvested power density. It was found that the open circuit voltage of 0.1 wt.% AgNWs contained films was 52% higher than that of pure PVDF-HFP films. Furthermore, the harvested power density was increased by 159%. Overdose of AgNWs resulted in crystal defects and the lower degree of crystallinity, leading to the relatively worse piezoelectricity.

1 Introduction

Poly(vinylidene fluoride)(PVDF) and its copolymers have become promising materials for self-powered devices in recent decades because of their relatively high piezoelectricity, nontoxicity, and high resistance to halogen and acid. Furthermore, they are of high flexibility and durability, thus can be easily tailored and shaped for applications to various structures.[1,2] To date, many efforts have been made to fabricate self-powered devices based on PVDF or its polymers.[1,3-6]

PVDF is a semi-crystalline polymer possessing at least 5 polymorphs, i.e., *α*, *β*, *γ*, *δ* and *ε*. Among them, *α*-phase, with a non-polar trans-gauche-trans-gauche'(TGTG') conformation, is the most common one; while *β*-phase with a polar all trans(TT) conformation is the most important one since PVDF's piezoelectricity depends on its fraction and the alignment of dipole moment.[7] Therefore, increase of the *β*-phase fraction and reorientation of the dipole moment stand in the focus of the previous works for developing PVDF based materials of high piezoelectric performance.

To date, several methods were proposed to prepare PVDF films with high fraction of *β*-phase, such as stretching,[8] combination of stretching and poling,[7,9] high pressure crystallization.[10], etc. For instance, Li *et al*. studied the transformation from *α* to *β*-phase using stretching under different conditions.[8] The crystalline structure changes during the stretching process were observed by an optical tensile stress microscopy tester and the stretched films were investigated by a 3D digital microscope and an infrared microscope and Fourier transform infrared spectroscopy(FTIR). The study indicated that the stretching temperature T_s and elongation ratio λ apparently influenced the phase transformation from *α* to *β* crystal of PVDF. It was recommended that T_s around 100 ºC and λ above 3 were proper and the fraction of *β*-phase achieved over 90%. Moreover, poling also improves the formation of *β* polymorph.[7,9] Sencadas *et al*. investigated the *α* to *β*-phase transformation in stretching and poling. The films stretched at 80 ºC in an elongation ratio of 5 contained as high as 80% *β*-phase, which could be further improved by corona poling. Besides, it was also observed that the degree of crystallinity decreased with the increase of drawing ratio.[9] Simultaneous stretching and poling was also developed. Huan *et al*. applied a sinusoidal half-wave direct electric field during stretching the PVDF-HFP films (elongation ratio: 4.5).[11]The relationship between piezoelectric coefficient d_{33} and the poling electric field and temperature was studied. The electric field of 160 MV/m and the temperature of 65 ºC were proved to be the optimal conditions, under which d_{33} increased to 24 pCN^{-1}, i.e., about 10% higher than that of pure PVDF-HFP films.

Addition of nanofillers is another effective method to induce high *β*-phase content in PVDF films. In recent decades, various nanofillers, such as carbon nanotube(CNT), carbon nanofiber(CNF), graphene oxide, graphene,[12-15] were utilized as enhancing agents of *β*-phase. Wu *et al*. added CNT and CNF into PVDF to improve the piezoelectricity of PVDF.[12] It was observed that the fraction of *β*-phase increased significantly in CNT or CNF contained films, which was confirmed by X-ray diffraction (XRD). The open circuit voltage increased by 24% and 15% for the 0.05 wt.% CNT contained films and 0.05 wt.% CNF contained films, compared to that of pure PVDF films. The effect of CNT on the crystal structure and piezoelectricity was investigated by Lee *et al*.[13] PVDF/CNT composite films were

prepared by solution blending method, hot pressing and drawing by 400% elongation. It was confirmed by FTIR that the β-phase increased with the content of CNT and reached the maximum value at the optimal content (0.2 wt.%) and then decreased. It was concluded that CNT played a role as nucleate agent in the crystallization process thus induced the formation of β polymorph. The piezoelectric strain constant, i.e., d_{31}, increased by 10% at this optimal content. PVDF/graphene oxide nanosheets (GOn) composite films were fabricated by solution casting method by Achaby *et al*.[15] Purely piezoelectric β-phase films were obtained at 0.1 wt.% due to the high compatibility between GOn and the polymer. The enhancement mechanism was explained utilizing the density function theory (DFT) calculation carried out by Yu *et al*.[16] It is argued that the adsorption of molecular chains on the nanofiller surfaces may release energy, and during sonication, the α-conformation may retain some energies, thus the energy barrier between these two conformations is overcome, leading to the transformation from α-conformation to β-conformation. In situ reduction method was used to fabricate PVDF/rGO composite films by Rahman *et al*.[17] In this study, PVDF/GO films were prepared first, and then PVDF/rGO films were obtained by in situ thermal reduction of PVDF/GO films at 150 ºC. The peaks in XRD spectra related to α-phase almost disappear in PVDF/rGO composites, compared to that of neat PVDF films. In the energy harvested experiments, the output voltage of PVDF/rGO achieves 436 mV at the resonance frequency (i.e., 41 Hz), which is about 50% higher than that of pure PVDF films.

It is commonly recognized that nanofillers work as nucleating agents in the formation of β-phase during initial crystallization. However, the roles of nanofillers in the stretching and poling process have not been clearly uncovered to date. In this study, we added silver nanowires (AgNWs) into poly(vinylidene fluoride-co-hexafluoropropylene) (PVDF-HFP) to prepare composite films of excellent piezoelectricity. To the best of our knowledge, there is no work about the preparation of PVDF-HFP/AgNW films by solution casting method. Based on the investigation on crystal structures and the electrical output experiments, we clarified the roles played by AgNWs in phase transformation in the three steps, i.e., initial crystallization, stretching and poling. The positive effect of moderate addition of AgNWs on the β-phase formation and the phase transformation was proved, meantime the negative effect of overdosed AgNWs which decreased the crystallinity degree was also observed. Thus, a balance for improving the β-phase formation and phase transformation, and maintaining high crystallinity degree was pursued, i.e., the optimal content of AgNWs, which was obtained by adding different contents of AgNWs. The improvement of piezoelectricity was confirmed by the increase of open circuit voltage and power harvesting experiments.

2 Experiments

2.1 Materials

Poly(vinylidene fluoride-hexafluoropropylene) (PVDF-HFP) (Kynar Flex 2801) and N,N-dimethylformamide (DMF) were commercially obtained and used as received. The properties of PVDF-HFP are showed in Table 1.

AgNW was synthesized by a hydrothermal synthetic method as reported previously.[18] AgNW was in suspended state in ethanol after synthesis, and the ethanol was replaced by DMF to avoid porous in films (ESI-1). Microstructure of AgNWs was characterized by TEM (JEM-2100F). Figs. 1(a) and 1(b) show the bright-field TEM images of the AgNWs. The nanowires are straight and their diameters range from 150 nm to 250 nm. Fig. 1(c) shows a diffraction pattern of the AgNWs, which can be indexed as the diffraction of FCC-Ag along its [110] zone axis. Fig. 2 is an EDS spectrum of the AgNWs. The C and Cu signals come from the carbon mesh supporting the AgNWs for TEM characterization.

Table 1 Properties of PVDF-HFP

Density	1.76~1.80 gcm^{-3}
Refraction index	1.41
Melting Temperature	140~145°C
Melt viscosity (232°C, 100 s^{-1})	2300~2700 Pa·s
Water absorption (23°C,24h)	0.03%
Melt flow rate (232°C, 125 kg)	0.35~0.75 $gmin^{-1}$

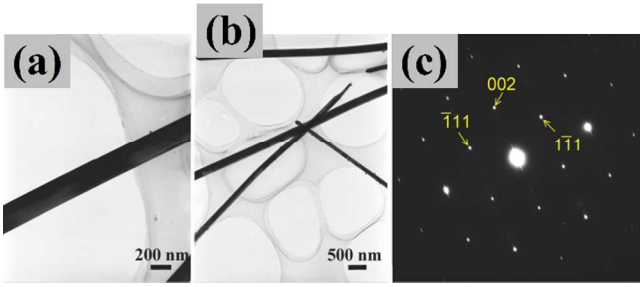

Fig. 1 TEM images (a) ×30k (b) ×10k and SEAD pattern of AgNW

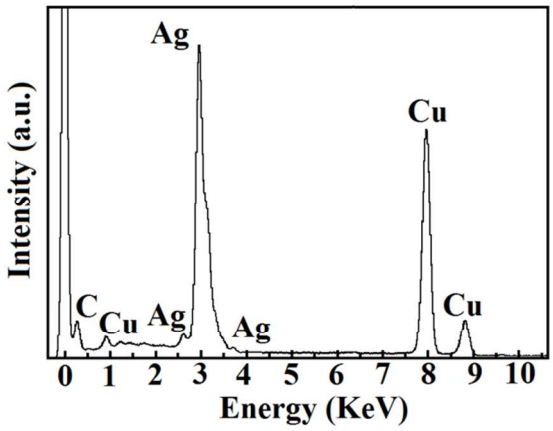

Fig. 2 Energy dispersive spectrometer (EDS) spectrum of AgNW

2.2 Preparation of PVDF-HFP/AgNW composite films

The detailed information of preparation process is in our previous work[12] or in supplemental files (ESI-2). Here, we only provided a simplified description: (a) Preparation of AgNW/DMF suspension; (b) Solution of PVDF-HFP in AgNW/DMF (PVDF-HFP:DMF=1:3) suspension by sonication and mechanical stirring; (c) crystallization on Al plate at 90 ºC; (d) Stretching at about 65 ºC (elongation ratio:4~5); (d) Poling by step-wise method in

silicon oil, and the maximum electric field is 70 MVm^{-1}.

Before poling, two electrodes were bonded on both sides of a film by conductive epoxy, for FTIR, POM and DSC characterizations of poled films, the conductive epoxy was removed by immersing the specimens in ethanol for two days.

Fig. 3 is the images of PVDF-HFP/AgNW composite films. It can be observed that the films containing AgNW are of silver gray, and the colour becomes darker with the increase of AgNW content. Compared to untreated films, the stretched films are more transparent. The stretched/poled films (not shown) are similar to the stretched films. Besides, pure PVDF-HFP films with or without stretching and poling were also made as additional experiments to investigate the roles of stretching and poling, their piezoelectricity was evaluated by measuring their open circuit voltages.

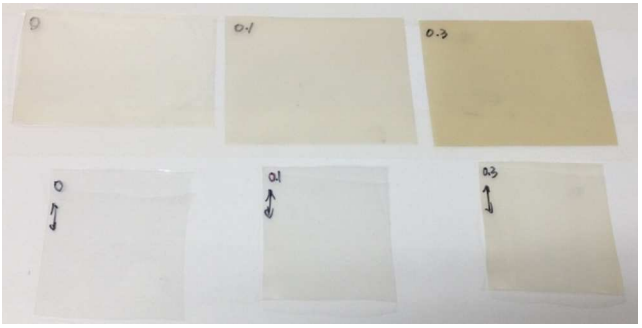

Fig. 3 Untreated and stretched films (The arrow indicates the stretching direction). The more AgNWs contained, the less transparent. Compared to untreated films, the stretched films are more transparent.

Table 2 shows the average thicknesses of various PVDF-HFP/AgNW films. For simplicity of description, the composite films are named as PVDF-HFP, PVDF-HFP/AgNW(0.05), PVDF-HFP/AgNW(0.1), PVDF-HFP/AgNW(0.2), PVDF-HFP/AgNW(0.3) corresponding to the AgNW contents of 0.0 wt.%, 0.05 wt.%, 0.1 wt.%, 0.2 wt.% and 0.3 wt.%, respectively.

Table 2 Thicknesses of stretched PVDF-HFP/AgNW composite films

AgNW content (wt.%)	0	0.05	0.1	0.2	0.3
Average thickness (μm)	73.40	74.63	73.04	68.89	71.74
Standard deviation (μm)	5.54	4.20	7.68	4.05	4.05

2.3 Electrical experiments

The present experimental setup is shown in Fig. 4. The fabricated films were cut into rectangle pieces of sizes of 3 cm (stretching direction) and 2.5 cm and then attached to an Al plate by epoxy at 25 ºC(ESI-3). An amplified sinusoidal voltage generated by a function generator excited an electromagnet located at the bottom surface of the Al plate, resulting in dynamic strains in the piezoelectric film. The generated voltage in the films was measured by an oscilloscope and used for evaluating the piezoelectricity. Due to significant influence of exciting frequency on the output voltage, in the present experiments, all samples worked near the first resonance frequency of the plate, i.e., 26.5 Hz. It should be noted that in the open circuit voltage experiments, the films were independent, the displacement of the free end of the Al plate was adjusted to 1 mm, while in power harvesting experiments, they were in parallel and the displacement was 1.5 mm.

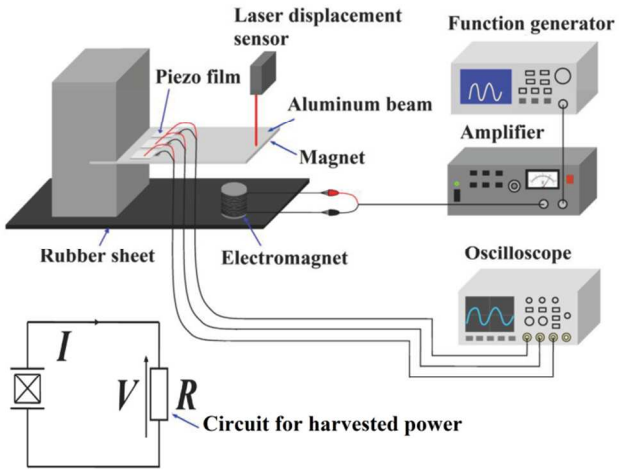

Fig. 4 Experiment Setup

2.4 Characterization of PVDF-HFP/AgNW composite films

In order to investigate the structure change of composite films in initial crystallization, stretching and poling processes, analyses of polarized optical microscope (POM), FTIR and differential scanning calorimetry (DSC) were performed.

2.4.1 POM

The composite films were cut into 10 μm thick specimens by a microtome (Leica Microsystems, RM 2145) for the morphology observation by a POM (Eclipse model ME600D). The specimens were cut along the thickness direction and the cross section was observed.

2.4.2 FTIR

FTIR was carried out by an FTIR instrument(IRT-7000, Jasco, Japan) within the wavenumber ranging from 400 cm^{-1} to 4000 cm^{-1}. The samples contained AgNW at 0.0 wt.%, 0.1 wt.% and 0.3 wt.% at the three stages (untreated, stretched, stretched/poled) were investigated.

2.4.3 DSC

In order to investigate the degree of crystallinity in the composite films, DSC was also performed by a Diamond DSC machine (PerkinElmer Instruments). A sample was held at 40 ºC and then heated from 40 ºC to 200 ºC at 10 ºCmin^{-1} in nitrogen atmosphere. The melting enthalpy was calculated by a DSC analysis software, i.e., Pyris.

3 Results and Discussion

3.1 Electrical experiments

3.1.1 Open circuit voltage

For simplicity, we make following definition about coordinate

directions: *3* represents the thickness direction, for stretched films, *1*denotes the stretching direction and *2* denotes the direction perpendicular to *1*. For untreated films, *1* denotes an arbitrary direction in the film plane and *2* denotes the direction perpendicular to *1* (ESI-4). In our experiments, the films work in *31* mode.

As the output voltage is proportional to the plate tip displacement and the film thickness.[12] Considering the small variation of tip displacement and thickness of each sample, we use the following equation to calculate calibrated open circuit voltage.

$$V_c = V\frac{u_0 t_0}{ut} \quad (1)$$

where u is the tip displacement of the Al plate, t the thickness of the tested films, and u_0 (1 mm) and t_0 (100 μm) are the standard displacement and standard thickness, respectively.

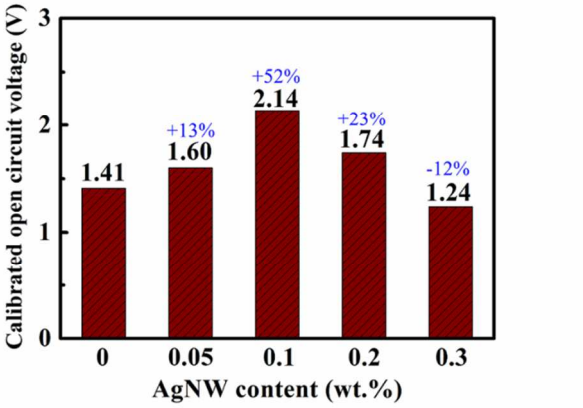

Fig. 5 Calibrated open circuit voltage of PVDF-HFP/AgNW composite films

Fig. 5 shows the calibrated open circuit voltage of PVDF-HFP/AgNW composite films. In this figure, the calibrated voltage of PVDF-HFP/AgNW(0.1) composite films is 2.14 V, i.e., around 52% higher than that of pure PVDF-HFP films, indicating the significant improvement effect by AgNW on PVDF-HFP's piezoelectricity. However, overdose of AgNWs has a negative effect, in this figure, the films containing AgNWs over 0.1 wt.% generate relatively lower voltages. It attributes to the influences of AgNWs on the phase transformation and the reorientation of dipole moments during the preparation of composite films, as discussed in Section 3.2.

3.1.2 Harvested power

The density of power is calculated by

$$D_p = \frac{V^2}{V_{ol}R} \quad (2)$$

in which V is the voltage on the load resistance, V_{ol} the total volume of three films and R is the load resistance.

Fig. 6 demonstrates the density of harvested power. Compared to pure PVDF-HFP films, the density of harvested power of PVDF-HFP/AgNW(0.1) is 10.16 Wm^{-3}, which is 159% higher than that of pure PVDF-HFP films. When the AgNW content is over 0.1 wt.%, the density of harvested power decreases, which is consistent with the trend of open circuit voltage.

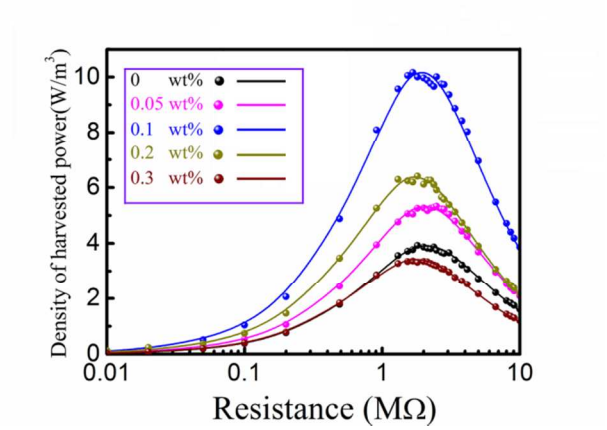

Fig. 6 Density of harvested power of PVDF-HFP/AgNW composite films

The present result was further analysed by the model proposed by Guyomar *et al.*[19] According to the model, the density of harvested power is expressed as

$$D_p = \frac{R\alpha^2}{1+(RC_0\omega)^2}\frac{F_m^2}{2V_{ol}C^2} \quad (3)$$

$$R_{opt} = \frac{1}{C_0\omega} \quad (4)$$

where R is the load resistance, α the force factor, F_m the external force applied on the films, C_0 the clamped capacitance of the films, ω the frequency, and C is the damping ratio corresponding to the mechanical losses of the structure.

Thus, the maximum density of harvested power is

$$D_{pmax} = \frac{\alpha^2}{4C_0\omega}\frac{F_m^2}{V_{ol}C^2} \quad (5)$$

The force factor α and the capacitance of films C_0 can be calculated by

$$\alpha = e_{31}w \quad (6)$$

$$C_0 = \frac{\varepsilon A}{t} = \frac{\varepsilon_r\varepsilon_0 wl}{t} \quad (7)$$

where e_{31} the piezoelectric constant, w the width of the film, ε the permittivity of the piezoelectric element, ε_r the dielectric constant, ε_0 the permittivity of free space (8.85×10^{-12} Fm^{-1}), l the length of the film, and t is the film thickness.

Therefore, we can obtain

$$\varepsilon_r = \frac{C_0 t}{\varepsilon_0 wl} \quad (8)$$

The power density constant for the structure is defined as

$$C_{pd} = \frac{\alpha^2 F_m^2}{2V_{ol}C^2} \quad (9)$$

By using Eqs. (3) and (4), the density of harvested power can be expressed as

$$D_p = \frac{R}{1+\left(\frac{R}{R_{opt}}\right)^2}C_{pd} \quad (10)$$

As the density of harvested power stays on a high platform for a wide range of resistance, it is difficult to directly determine the accurate optimal resistance from Fig. 6. Nevertheless, from Fig. 6, it is obvious that the approximate R_{opt} is about 2 MΩ, which is much larger than 0.05MΩ (a measureable lower limit), so the power at 0.05 MΩ and R_{opt} can be calculated as

$$D_{pR0.05} = 0.05\ C_{pd},\quad D_{pRopt} = \frac{R_{opt}}{2} C_{pd} \tag{11}$$

Therefore

$$R_{opt} = \frac{0.1 D_{pRopt}}{D_{pR0.05}} \tag{12}$$

By utilizing Eq. (12), R_{opt} can be approximately estimated with measured $D_{pR0.05}$ and D_{pRopt}, and C_{pd} can be calculated.

To further accurately identify R_{opt} and C_{pd}, we changed R_{opt} in the interval (0.97 R_{opt}, 1.03 R_{opt}). By comparing with experimental data, we determined the group of R and C_{pd} of the lowest error rate as R_{opt} and C_{pd}. After determining R_{opt}, C_0 can be calculated by Eq. (4). The results are summarized in Table 3.

Table 3 Parameters of harvested power experiments

Content (wt.%)	0	0.05	0.1	0.2	0.3
R_{opt}(MΩ)	2.08	2.04	1.93	1.72	1.75
C_{pd}(10^{-6}WΩ^{-1}m^{-3})	3.76	5.22	10.45	7.42	3.91
Error rate (%)	±3.2	±3.3	±3.2	±2.9	±3.3
D_{pmax}(Wm^{-3})	3.92	5.33	10.16	6.41	3.36
C_0(pF)	2887	2944	3112	3492	3432
$^aC_{0m}$ (pF)	2950	3100	3180	3390	3420
ε_r	10.87	11.62	11.66	11.73	12.32

$^aC_{0m}$ is the capacitance measured by a multi-meter directly.

The experimental results show the validity of the model proposed by Guyomar *et al*.[19] Based on the results, we can conclude that the optimal resistance decreases with the increase of AgNW content, according to Eq. (4), the capacitance increases. This trend is consistence with the direct measurements by a multi-meter(see Table 3). The permittivity calculated by direct measurements increases with AgNW content, indicating the addition of conductive filler may lead to higher permittivity.[17,20]

From Table 3, $C_{pd\text{-}0.1}$ is about 3 times of $C_{pd\text{-}0}$. As a low content of metallic nanowires can only influence the PVDF-HFP's Young's modulus slightly at room temperature,[21] the external force F_m is considered unchanged. By neglecting the small variation of volume V_{ol} and damping ratio C, it is argued that the increase of C_{pd} is mainly attributed to the increase of force factor α (Eq. (9)), i.e., the piezoelectric constant e_{31} (Eq. (6)).

3.2 Characterization of PVDF-HFP/AgNW composite films

3.2.1 POM

Fig. 7 illustrates the POM images of PVDF-HFP/AgNW composite films. For simplicity, U, S and SP in Figs. 7 and 8 denote untreated films, stretched films and stretched/poled films, the number is the AgNW content (wt.%). Aapparently, in the untreated films (Figs. 7(a), 7(b), 7(c)), films crystallized in spherulitic structures. Furthermore, in pure PVDF-HFP films, there are various sizes of spherulitic structures. In PVDF-HFP/AgNW(0.1) films, the crystal size seems to be larger and the spherulitic crystal density is lower. It is more obvious in PVDF-HFP/AgNW(0.3) films, in which the spherulitic crystal density is dramatically reduced. As the spherulitic structures reflect the existence of α-phase,[23,24] thus it is argued that after addition of AgNWs, the content of α-phase decreased significantly even the films are not stretched. It implies that the content of β-phase increased in initial crystallization stage, which is in consistent with the results of FTIR spectra. The mechanism of β-phase formation may be due to the adsorption of molecule chains on the surface of nanofillers, as the simulation carried by Yu *et al*.[16] They applied DFT(density of function theory) to calculate the adsorption energies of α-chains and β-chains on the surface of carbon nanotubes. It was reported that the released energy of β-chains is 0.2 eV higher than that of α-chains. Thus during adsorption, the energy barrier between α-polymorph and β-polymorph may be overcome, leading to the increase of β-phase and decrease of α-phase. Such β-phase formation may occur on AgNWs surfaces. However, overdose of AgNWs may cause more crystal defects, which results in initial stresses in crystals, leading to the decrease of crystallinity degree.[22] In addition, too many nucleating centers also confine the movement of molecular chains.

In stretched films (Figs. 7(d), 7(e), 7(f)), the spherulitic crystalline structures turned into fiber-like structure along the stretching direction, especially in the films contained 0.1 wt.% AgNWs. The alignment of molecular chains promotes the transformation from α to β-phase.[24,26]

Comparing the images of stretched films with those of stretched/poled films, there is no apparent difference, indicating the effect of poling on the morphology is limited. In fact, poling mainly contributes to the reorientation of dipole moment of β-phase, as discussed in Section 3.2.2.

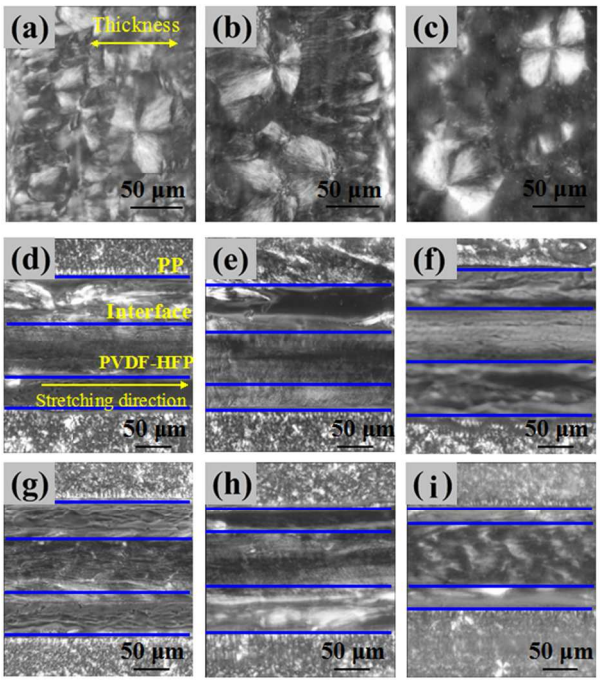

Fig. 7 POM images of PVDF-HFP/AgNW composite films:(a)0U;(b)0.1U;(c)0.3U;(d)0S;(e)0.1S;(f)0.3S;(g)0SP;(h)0.1SP;(i)0.3SP.

3.2.2FTIR analysis

Fig. 8 shows the FTIR spectra of PVDF-HFP/AgNW composite films. From Fig. 8, it is obvious that AgNWs influence the phase transformation dramatically in initial crystallization process. In untreated films, the peaks corresponding to α-phase, i.e., the peaks at 615 cm^{-1}, 763 cm^{-1} and 975 cm^{-1} are obvious. With the increase of AgNW content, the peaks become weaker, while the peak at 840 cm^{-1} corresponding to β-phase increases.[7] This indicates that the addition of AgNWs can induce the formation of β-phase in the initial crystallization. In stretched films, the peaks corresponding to α-phase decrease, especially for the films contained AgNWs less than 0.1 wt.%. Here, we stretched the films at about 65°C, it is a proper temperature for the formation of β-phase and a higher temperature may lead to lower fraction of β-phase.[8] As the fraction of β-phase of PVDF-HFP/AgNW(0.3) films is quite high before stretching, so the effect of stretching and poling is not so obvious in this case.

The relative fraction of β-phase, i.e., $F(\beta)$ is calculated by

$$F(\beta) = \frac{A_\beta}{1.26A_\alpha + A_\beta} \quad (13)$$

where A_α and A_β are the absorbencies at 763 cm^{-1} and 840 cm^{-1}, respectively.[8]

Table 4 shows the relative fraction of β-phase, reflecting phase transformation of all samples in the whole preparation process.

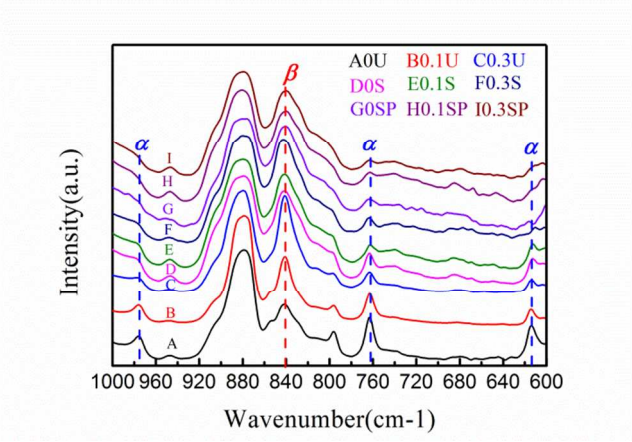

Fig.8 FTIR spectra of PVDF-HFP/AgNW composite films

Table 4 Relative fraction of β-phase in PVDF-HFP/AgNW films

Content (wt%)	0	0.1	0.3
Untreated	58%	73%	87%
Stretched	82%	89%	90%
Stretched and Poled	89%	92%	94%

From Fig. 8 and Table 4, we can conclude that all the three factors, i.e., the addition of AgNWs, stretching and poling, influence the crystal structure. For untreated films, $F(\beta)$ increases with the increase of AgNW content and reaches 87% in PVDF-HFP/AgNW(0.3) films. For stretched films, the influence of stretching on inducing of β-phase films containing low content of AgNWs is significant, but not so obviously in PVDF-HFP/AgNW(0.3) films. From Table 4, we can see that in stretched PVDF-HFP/AgNW(0.1) films, the content of β-phase is as high as 89%, indicating that most α-phase has been transformed. This can be confirmed from Fig. 8, in which the characteristic peaks of α-phase nearly disappear. Therefore, moderate addition of AgNWs may play an important and positive role in the phase transformation caused by stretching. It was reported that nanofillers may work as nucleating agents, resulting in rapid crystallization.[7] Furthermore, the stress concentration on AgNWs may promote the extension of molecule chains, thus the β-phase of the highest density becomes the favourite polymorph.[27] However, in the films with overdosed AgNWs, the effect is not so significant. Similarly, poling plays an important role in pure PVDF-HFP films, but has a relative weaker effect in AgNW contained films. Generally speaking, when compared to the films of low content of AgNWs, since $F(\beta)$ is quite high at initially crystallized PVDF-HFP/AgNW(0.3) films, the effects of stretching and poling are relatively weaker.

3.2.3 DSC

Fig. 9 shows the DSC thermograms of PVDF-HFP/AgNW composite films after stretching and poling (Temperature range: 60 ºC to 180 ºC). From Fig. 9, the melting temperature slightly decreases with the increase of AgNW content, which may be attributed to the crystallinity change or local influence of the polymer conformation related to AgNW.

The crystallinity degree is calculated by[28]

$$X_c = \left(\frac{\Delta H_m}{\Delta H_m^\emptyset}\right) \times 100\% \quad (14)$$

where ΔH_m is the melting enthalpy of the composite film which is calculated by the DSC analysis software Pyris and $\Delta H_m^\emptyset$ is the melting enthalpy of pure crystalline material, i.e., 104.50 Jg^{-1}.

Table 5 shows the DSC results of the samples containing different contents of AgNW. It is worth noting that a small addition of AgNW may increase the crystallinity degree, however, for the case of 0.3 wt.% AgNW, the crystallinity degree decreases dramatically, when compared to that of optimal content. As a result, the films with overdosed AgNWs may perform worse compared to neat PVDF-HFP films.

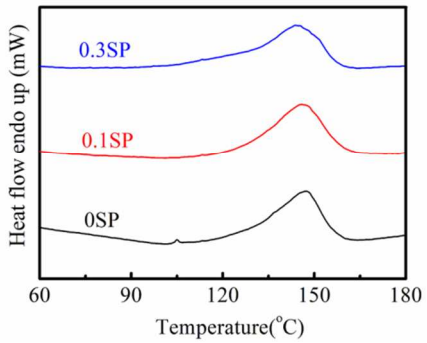

Fig. 9 DSC thermograms of PVDF-HFP/AgNW composite films

Table 5 DSC results of PVDF-HFP/AgNW composite films

Content (%)	0	0.1	0.3
T_m(℃)	147.21	145.63	143.70
ΔH_m(Jg^{-1})	24.00	28.84	20.48
X_c(%)	22.97	27.60	19.60

Table 6 Calibrated voltage of pure PVDF-HFP films under different conditions

Stretching	Poling	Calibrated voltage
√	√	1.4 V (a)
√	×	0.0 V (b)
×	√	0.2 V (c)
×	×	0.0 V (d)

3.2.4 Additional experiments

By combining with the results of open circuit voltage of pure PVDF-HFP films under different conditions, the effects of stretching and poling in fabricating piezoelectric films can be further explored. The calibrated voltages of pure PVDF-HFP films under different preparation conditions are summarized in Table 6. All the films without poling cannot generate voltage, indicating poling makes the dipole moments of piezoelectric β-phase along the poling direction. Comparing (a) and (c) in Table 6, it is concluded that stretching induces the phase transformation as well as forces the molecular chain align along the stretching direction.

3.3 Summary of phase transformation

The influences of nanofiller addition, stretching and poling are summarized as: (a) Addition of nanofiller induces the formation of β-phase in crystallization process; (b) Stretching induces the transformation from α- to β-phase and forces the molecular chain along the stretching direction; (c) Poling improves the transformation from α- to β-phase and makes the dipole moment of piezoelectric β-phase along the electric field direction; (d) In AgNW contained films, the effect of stretching and poling on phase transformation becomes weaker; (e) Overdosed AgNWs may cause crystal defects which leads to the decrease of crystallinity degree.

4 Conclusions

In this study, AgNW was added into PVDF-HFP/DMF solution to fabricate powerful piezoelectric PVDF-HFP/AgNW composite films. The open circuit voltage is raised by 52% and the content of β-phase reaches 94%. It was observed that AgNW influenced the phase formation significantly during the preparation. Moderate AgNW addition enhanced the piezoelectricity of PVDF-HFP significantly due to the role of nucleate agent played by AgNW, while the films containing overdosed AgNWs generated relatively lower voltages due to the negative effects of overdosed AgNW on the crystallinity degree. The phase transformation was investigated by POM, FTIR and DSC. It was concluded that both stretching and poling led to the α to β-phase transformation. However, for the films containing high contents of AgNWs, as the crystallized films already possessed relatively high fraction of β-phase, the influences of stretching and poling on phase transformation were not so obvious. In order to obtain the optimal content of AgNWs, we blended PVDF-HFP films with various contents of AgNWs. The experiments showed that when the AgNW content is 0.1 wt%, the promoting role of AgNWs on β-phase formation and phase transformation can be realized and the negative effect causing the lower crystallinity degree is limited. Thus, this content was determined as the optimal one.

Acknowledgements

This work is supported by the Research Funds from NSF of China (No. 11372104 and No. 51275466).

Notes and references

[a]*School of Aerospace Engineering, Chongqing University, Chongqing 400044, P. R. China Fax:+86-023-6510-2421; Tel: +86-023-6510-2527; E-mail: huning@faculty.chiba-u.jp or ninghu@cqu.edu.cn*
[b]*Department of Mechanical Engineering, Zhejiang University, Hangzhou 310027, P. R. China E-mail: wuliangke@zju.edu.cn*
[c]*Technical Institute of Physics and Chemistry, Chinese Academy of Sciences, Beijing 100190, P. R. China*
[d]*Department of Machine Intelligence and Systems Engineering, Akita Prefectural University, Akita 015-0055, Japan*
[e]*World Premier International Research Center, Advanced Institute for Materials Research, Tohoku University, Sendai 980-8577, Japan*
† Electronic Supplementary Information (ESI) available: [details of any supplementary information available should be included here]. See DOI: 10.1039/b000000x/
‡ Footnotes should appear here. These might include comments relevant to but not central to the matter under discussion, limited experimental and spectral data, and crystallographic data.

1 D. Kim, S. Hong, D. Li, H.S. Roh, G. Ahn, J. Kim, M. Park, J. Hong, T. Sung and K. No, *Rsc Adv.*, 2013, **3**, 3194-3198.
2 F. Liu, N. A. Hashim, Y. Liu, M.R.M. Abed and K. Li, *J. Membr. Sci.*, 2011, **375**, 1-27.
3 N.G. Elvin, A.A. Elvin and M. Spector, *Smart Mater. Struct.*, 2001, **10**, 293-299.
4 J. Granstrom, J. Feenstra, H.A. Sodano and K. Farinholt, *Smart Mater. Struct.*, 2007, **16**, 1810-1820.
5 S. Li, J. Yuan and H. Lipson, *J. Appl. Phys.*, 2011, **109**, 026104.
6 Y. Liu, G. Tian, Y. Wang, J. Lin, Q. Zhang and H.F. Hofmann, *J. Intell. Mater. Syst. Struct.*, 2009, **20**, 575-585.
7 G.H. Kim, S.M. Hong and Y. Seo, *Phys. Chem. Chem. Phys.*, 2009, **11**, 10506-10512.
8 L. Li, M. Zhang, M. Rong and W. Ruan, *RSC Adv.*, 2014, **4**, 3938-3943.
9 V. Sencadas, R. Gregorio, JR. and S. Lanceros-Méndez, *J. Macromol. Sci. Part B: Phys.*, 2009, **48**, 514-525.
10 J. Scheinbeim, C. Nakafuku, B.A. Newman and K.D. Pae, *J. Appl. Phys.*, 1979, **50**, 4399-4405.
11 Y. Huan, Y. Liu and Y. Yang, *Polym. Eng. Sci.*, 2007, **47**, 1630-1633.
12 L. Wu, W. Yuan, T. Nakamura, S. Atobe, N. Hu, H. Fukunaga, C. Chang, Y. Zemba, Y. Li, T. Watanabe, Y. Liu, Alamusi, H. Ning, J. Li, H. Cui and Y. Zhang, *Adv. Compos. Mater.*, 2013, **22**, 49-63.
13 J. S. Lee, G.H. Kim, W.N. Kim, K.H. Oh, H.T. Kim, S.S. Hwang and S.M. Hong, *Mol. Cryst. Liq. Cryst.*, 2008, **491**, 247-254.
14 R.K. Layek, S. Samanta, D.P. Chatterjee and A.K. Nandi, *Polym.*, 2010, **51**, 5846-5856.
15 M.E. Achaby, F.Z. Arrakhiz, S. Vaudreuil, E.M. Essassi and A. Qaiss, *Appl. Surf. Sci*, 2012, **258**, 7668-7677.
16 S. Yu, W. Zheng, W. Yu, Y. Zhang, Q. Jiang and Z. Zhao, *Macromol.*, 2009, **42**, 8870-8874.
17 M.A. Rahman, B. Lee, D. Phan and G. Chung, *Smart Mater. Struct.*, 2013, **22**, 085017.

18 N. Li, G. Huang, X. Shen, H. Xiao and S. Fu,*J. Mater. Chem. C*, 2013,**1**,4879-4884.

19 D. Guyomar, A. Badel, E. Lefeuvre and C. Richard, *IEEE Trans. Ultrason. Ferroelectr. Freq. Control*, 2005, **52**, 584-595.

20 W. Zheng, X. Lu, W. Wang, Z. Wang, M. Song, Y. Wang and C. Wang, *Phys. Status Solidi A*, 2010, **207**, 1870-1873.

21 B. Lin, G. A. Gelves, J. A. Haber and U. Sundararaj, *Ind. Eng. Chem. Res.*, 2007, **46**, 2481-2487.

22 W. Yu, Z. Zhao, W. Zheng, B. Long, Q. Jiang, G. Li and X. Ji, *Polym. Eng. Sci.*, 2009, **49**, 491-498.

23 R. Song, D. Yang and L. He, *J. Mater. Sci.*, 2007, **42**, 8408-8417.

24 D. Shah, P. Maiti, E. Gunn, D.F. Schmidt, D.D. Jiang, C.A. Batt and E.P. Giannelis, *Adv. Mater.*, 2004, **16**, 1173-1177.

25 Y. Song, Z. Zhao, W. Yu, B. Li and X. Chen, *Sci. China Ser. B: Chem.*, 2007, **50**, 790-796.

26 L. L. Sun, B. Li, Z.G. Zhang and W.H. Zhong, *Eur. Polym. J.*, 2010, **46**, 2112-2119.

27 BJ Jungnickel, *Poly (vinylidene fluoride)(overview) in: Salamone JC(Ed), Polymer Materials Handbook*, CRC Press Inc, 1999.

28 S. Lanceros-Méndez, J.F. Mano, A.M. Costa and V.H. Schmidt, J. Macromol. Sci.-Phys., 2001, B40, 517-527.